

The 8-h tide in the mesosphere and lower thermosphere over Maui (20.75° N, 156.43° W)

G. Jiang¹, J. Xu¹, and S. J. Franke²

¹State Key Laboratory of Space Weather, Center for Space Science and Applied Research, Chinese Academy of Sciences, Beijing, China

²Department of Electrical and Computer Engineering, University of Illinois at Urbana-Champaign, USA

Received: 6 October 2008 – Revised: 30 March 2009 – Accepted: 8 April 2009 – Published: 4 May 2009

Abstract. Wind data collected by the Maui meteor radar (20.75° N, 156.43° W) are used to study the 8-h tide in the mesosphere and lower thermosphere (MLT) region at a low-latitude station. The data set spans the time interval from 19 May 2002 to 24 May 2007. Our results show that the 8-h tide is a regular and distinct feature over Maui. The meridional component of this wave is significantly larger than the zonal component. The meridional component exhibits a semiannual variation in amplitude, with peaks near the equinoxes, whereas the variation of the zonal component does not show this seasonal characteristic. The strongest wave motions mostly occur in the height range of 92–96 km near spring equinox (March) and at higher altitudes near autumn equinox (October). The vertical variations of 8-h tidal phase at Maui indicate an upward wave energy flux. The vertical wavelengths are ≥ 54 km in equinox months.

Keywords. Meteorology and atmospheric dynamics (Middle atmosphere dynamics; Thermospheric dynamics; Waves and tides)

1 Introduction

The features and seasonal variabilities of the diurnal tide and semidiurnal tide in the mesosphere and lower thermosphere (MLT) have been quite well investigated through observations and model simulations (Manson and Meek, 1986; Teitelbaum et al., 1989; Thayaparan, 1997; Pendleton et al., 2000; Smith, 2000; Smith and Ortland, 2001; Akmaev, 2001; Younger et al., 2002; Batista et al., 2004; Namboothiri et

al., 2004; Taori et al., 2005; Zhao et al., 2005; Beldon et al., 2006; Tokumoto et al., 2007). Nevertheless, the 8-h tide, as a distinct wave signature in the MLT region, is not well understood, especially compared to the diurnal tide and semidiurnal tide. Besides the work of Smith (2000) based on the wind measurement of High Resolution Doppler Interferometer (HRDI) instrument on the Upper Atmosphere Research Satellite (UARS), the variations of the 8-h tide have been investigated using ground-based observations in the Northern Hemisphere at middle- and high-latitude (Manson and Meek, 1986; Teitelbaum et al., 1989; Thayaparan, 1997; Pendleton et al., 2000; Younger et al., 2002; Namboothiri et al., 2004; Taori et al., 2005; Zhao et al., 2005; Beldon et al., 2006). These studies showed that the seasonal behavior of the 8-h tide in the MLT region is different at different latitudes. For example, maximum amplitudes of the 8-h tide in the Northern Hemisphere were observed in the autumn (September–October) at the high-latitude station Esrange (68° N) (Younger et al., 2002), in autumn and early winter (September–November) at Castle Eaton, UK (52.6° N, 2.2° W) (Beldon et al., 2006), in winter and early spring (January–March) at Garchy (47° N), Montpazier (44° N) and London, Canada (43° N) (Teitelbaum et al., 1989; Thayaparan, 1997), and in winter (December–February) at Wakkanai (45.4° N) (Namboothiri et al., 2004). Overall, the 8-h tides at mid-latitude stations in the Northern Hemisphere have similar seasonal features, with maximum amplitudes in the winter months.

Recently, the characteristics of the 8-h tide over Cachoeira Paulista, Brazil (22.7° S, 45° W) were reported by Batista et al. (2004) and Tokumoto et al. (2007). At this low-latitude Southern Hemisphere site, the 8-h tide in the meridional wind peaked near the equinoxes (February–April and August–October) (Batista et al., 2004; Tokumoto et al.,



Correspondence to: G. Jiang
(gyjiang@spaceweather.ac.cn)

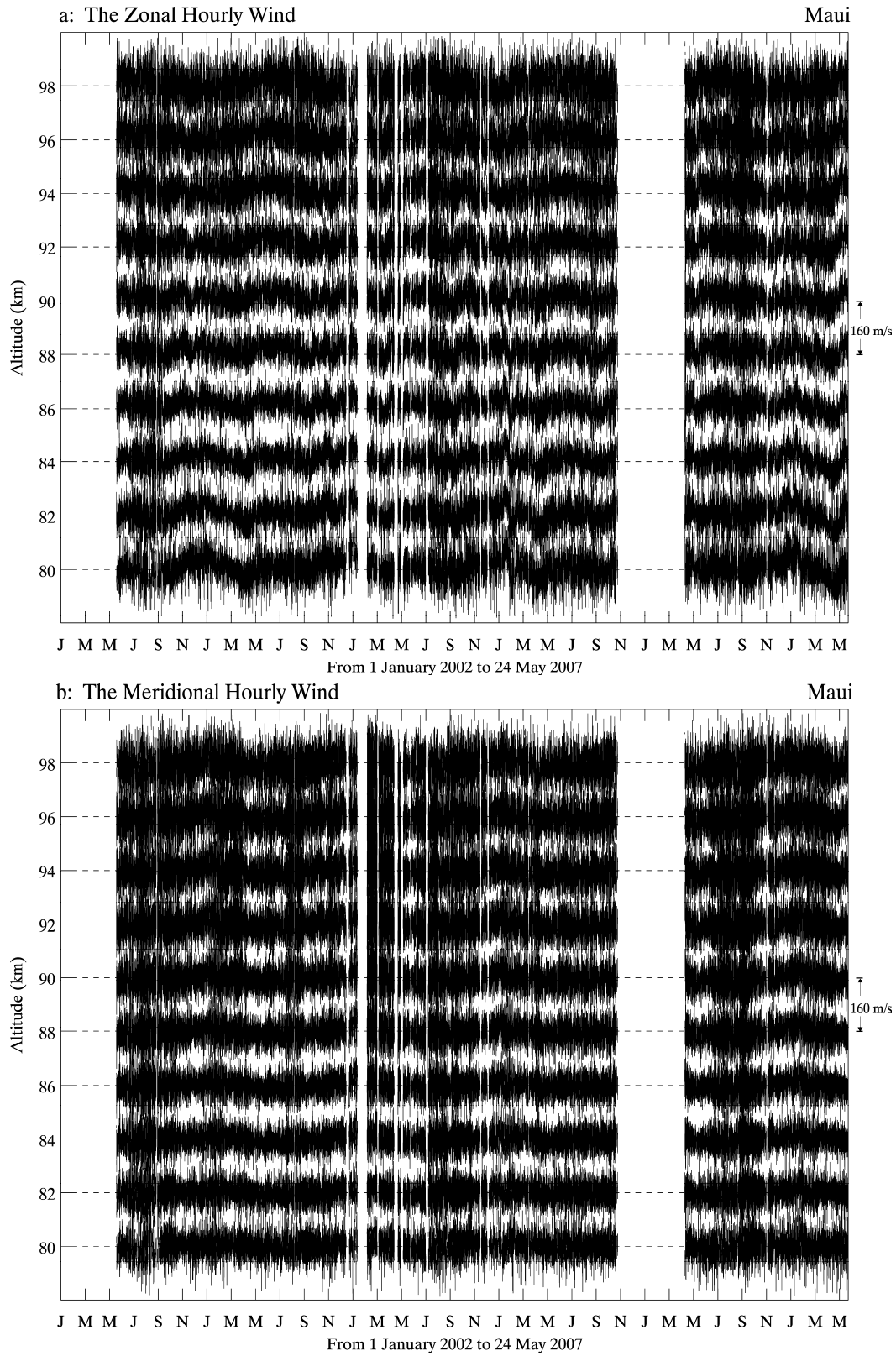


Fig. 1. The distributions of the hourly wind data with time and altitude. The plots (a) and (b) are for the zonal wind and the meridional wind, respectively.

2007). The HRDI/UARS satellite observations indicated that the 8-h tide amplitude was largest during autumn-middle winter at mid-latitude (Smith, 2000).

The phase variation and the vertical wavelength of the 8-h tide in the MLT region have also been found to differ between the zonal and meridional components, and at different locations. For example, regular annual variation of the wave phase was observed in the meridional wind at Wuhan (30° N) and Wakkanai (45.4° N) (Namboothiri et al., 2004; Zhao et al., 2005), and in the zonal wind at London, Canada (43° N) (Thayaparan, 1997). The vertical wavelength reported by the previous studies was found to vary widely, over a range from 12 to more than 1000 km. At high-latitude, 68° N, the vertical wavelength was from 31 km to 91 km (Younger et al., 2002); at mid-latitudes, ~43–52° N, the vertical wavelength varied in a large range from 22 to ≥ 1000 km (Thayaparan, 1997; Namboothiri et al., 2004); and at the low latitude of 22° S shorter vertical wavelengths ~12–32 km in the meridional wind were reported by Tokumoto et al. (2007).

At this time, the 8-h tide in the MLT region is still not well understood. As mentioned above, the 8-h tide at a low-latitude Southern Hemisphere site (22.7° S) displayed different climatological characteristics than the wave at mid- and high-latitudes in the Northern Hemisphere. In this paper we will present the features of the 8-h tide in the MLT region at a low-latitude site in the Northern Hemisphere, over Maui (20.75° N, 156.43° W), obtained from analysis of wind data collected by the Maui meteor radar from 19 May 2002 to 24 May 2007. The radar and data analysis methods are described in Sect. 2. The features of the 8-h tide over Maui are shown in Sect. 3. The comparisons between Maui 8-h tide and other observational and numerical results are discussed in Sect. 4. The main results of our study are summarized in Sect. 5.

2 Description of radar and data analysis

The Maui meteor radar was located in Kihei on Maui (20.75° N, 156.43° W), Hawaii. The system is a SKiYMET radar (Hocking et al., 2001) and operates at 40.92 MHz. A single three-element Yagi antenna directed toward the zenith is used to illuminate meteor trails. Meteor trail reflections are coherently detected on five three-element Yagi antennas oriented along two orthogonal baselines, with one antenna in the center of the array common to both baselines. On each baseline the outer antennas are separated from the center antenna by 1.5 and 2.0 wavelengths. This configuration minimizes antenna coupling, provides enough redundancy to unambiguously determine the azimuth and elevation of most echoes, and provides excellent angular resolution for position determination. The average transmitted power is approximately 170 W, resulting from a 13.3 μ s pulse length, 6 kW peak envelope power, and an interpulse period (IPP) of 466 μ s. Returns are sampled every 13.3 μ s, resulting in 2 km range res-

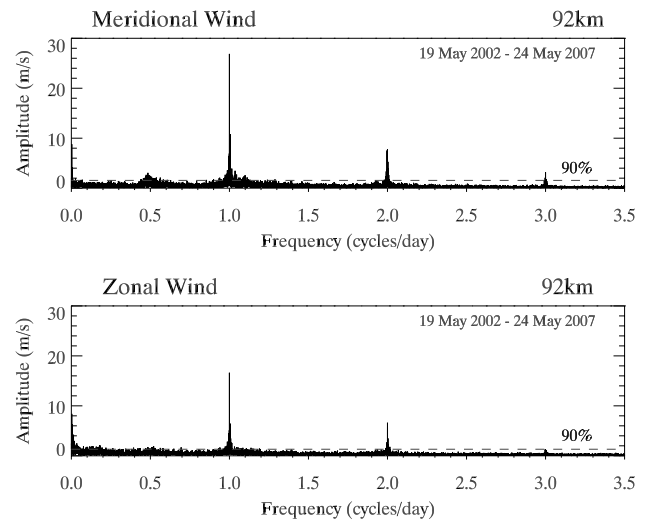


Fig. 2. Lomb-Scargle periodogram of the meridional wind (the top) and the zonal wind (the bottom) at 92 km from 19 May 2002–24 May 2007. The dashed line denotes the 90% confidence level.

olution. The relatively high PRF causes meteor echoes to be range aliased; however, the relatively narrow height distribution of meteor echoes combined with precise azimuth and elevation angle determination allows any range ambiguities to be resolved. The algorithms used to determine the meteor trail position and Doppler shift are described in detail in the work of Hocking and Thayaparan (1997). Wind velocities are estimated from the trail positions and Doppler shifts using a weighted least squares fit to an assumed constant wind vector composed of eastward and northward components. (The vertical wind is assumed to be negligible.) The wind vector fit is based on echoes collected within 1 h time bins. The more detailed description of Maui meteor radar and method of wind determination can be found in Franke et al. (2005).

The hourly wind data used in this paper are in the height range 80–98 km, and span a period of 5 years from 19 May 2002–24 May 2007, during which there are some short gaps and one significant gap (greater than 1 month) from late October 2005 to early April 2006. Figure 1 shows the distributions of the hourly wind data with time and altitude. The plots a and b are for the zonal wind and the meridional wind, respectively.

The Lomb-Scargle periodogram method (Lomb, 1976; Scargle, 1982) is used to determine which waves are dominant in the meridional and zonal wind. The advantage of this method is that it can accept the unevenly sampled input data. Hence the Lomb-Scargle periodogram method is widely applied to analyze geophysical data sets.

The harmonic fitting method with 4-day window sliding forward by 1 day is used to get the detailed information of the amplitude and phase of 2-day wave, diurnal tide, semidiurnal tide and 8-h tide. The 4-day fitting window is selected to

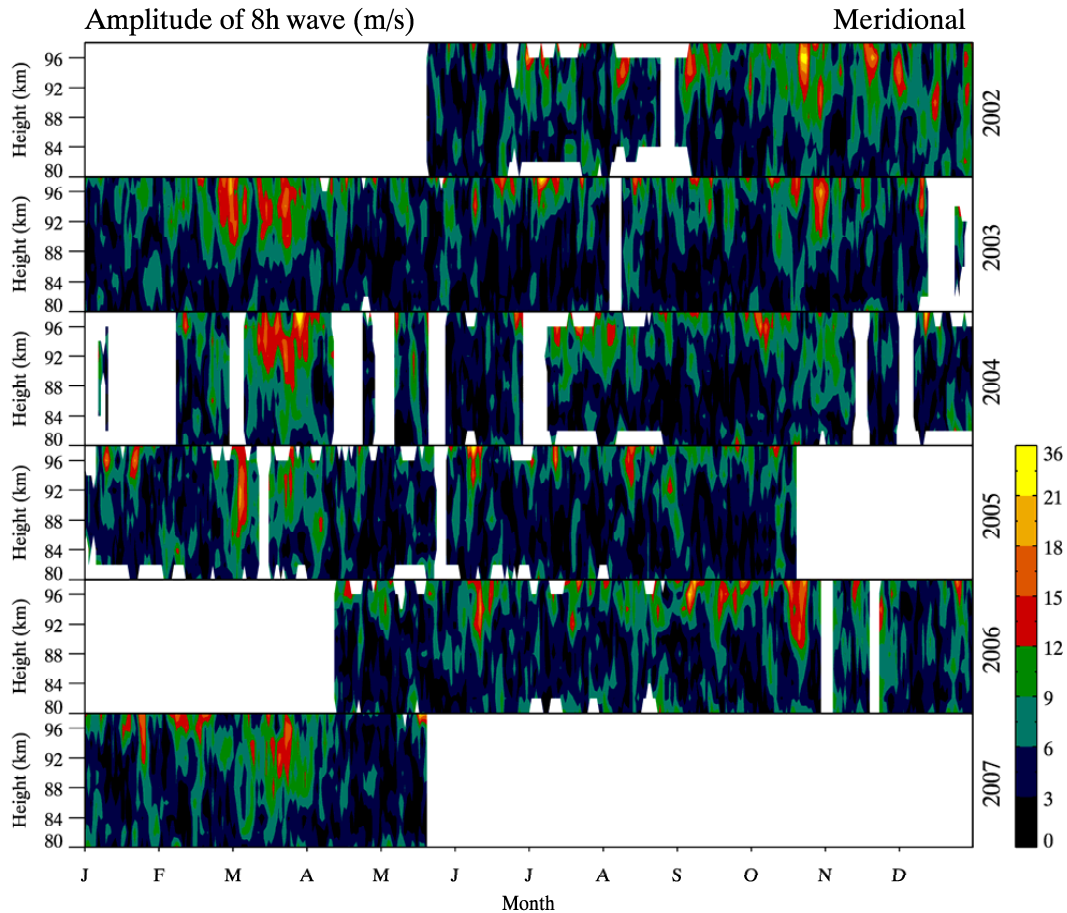


Fig. 3. Amplitude of the 8-h tide in the meridional wind from 19 May 2002–24 May 2007. The white blank represents no amplitude calculated from harmonic analysis because of no data or insufficient data for fitting.

remove the influence of 2-day wave, diurnal tide and semidiurnal tide, because these waves are usually particularly significant during some months, such as the very strong diurnal tide in the equinox near 20° N (Fritts and Isler, 1994). The fitting function used for harmonic analysis is

$$y(t) = \bar{y}(t) + \sum_{k=1}^4 A_k \cos\left(\frac{2\pi}{T_k}t + \phi_k\right) + R(t) \quad (1)$$

Where t is the local time; $y(t)$ is the wind data; $\bar{y}(t)$ is the prevailing component; A_k and ϕ_k are the amplitude and phase of the k -th harmonic component with a period of T_k ($T_1=48$ h, $T_2=24$ h, $T_3=12$ h and $T_4=8$ h). $R(t)$ denotes the residual. To ensure representative fits for each window, the wave amplitude and phase were calculated only when the number of valid data points was equal to or greater than 3/4 of the window length, i.e., when at least $3/4 \times (4 \times 24) = 72$ hourly wind estimates were available. Because the Lomb-Scargle periodogram method and the harmonic analysis can be applied to the unevenly sampled time series, no special treatment of data gaps was necessary.

3 Results

3.1 Tides in the MLT region over Maui

Figure 2 shows Lomb-Scargle periodogram of the meridional wind (the top) and zonal wind (the bottom) at 92 km from 19 May 2002 to 24 May 2007. As seen from this figure, the diurnal tide is the first dominant oscillation in the MLT region over Maui, and the semidiurnal tide is the second; however, they are beyond the scope of this paper. We will focus on the variations of 8-h tide. As shown in Fig. 2, the 8-h tide in the meridional wind is significant above the 90% confidence level during the whole period. Hence 8-h tide can be regarded as one of the dominant waves over Maui, a low-latitude site of Northern Hemisphere. The meridional component of 8-h tide is larger than the zonal component at 92 km. In fact, this phenomenon generally exists in the whole height range of 80–98 km.

First, let us discuss why the 8-h oscillation in Fig. 2 should be regarded as a manifestation of a tide, and not an inertia gravity wave or Lamb wave. There are two main reasons:

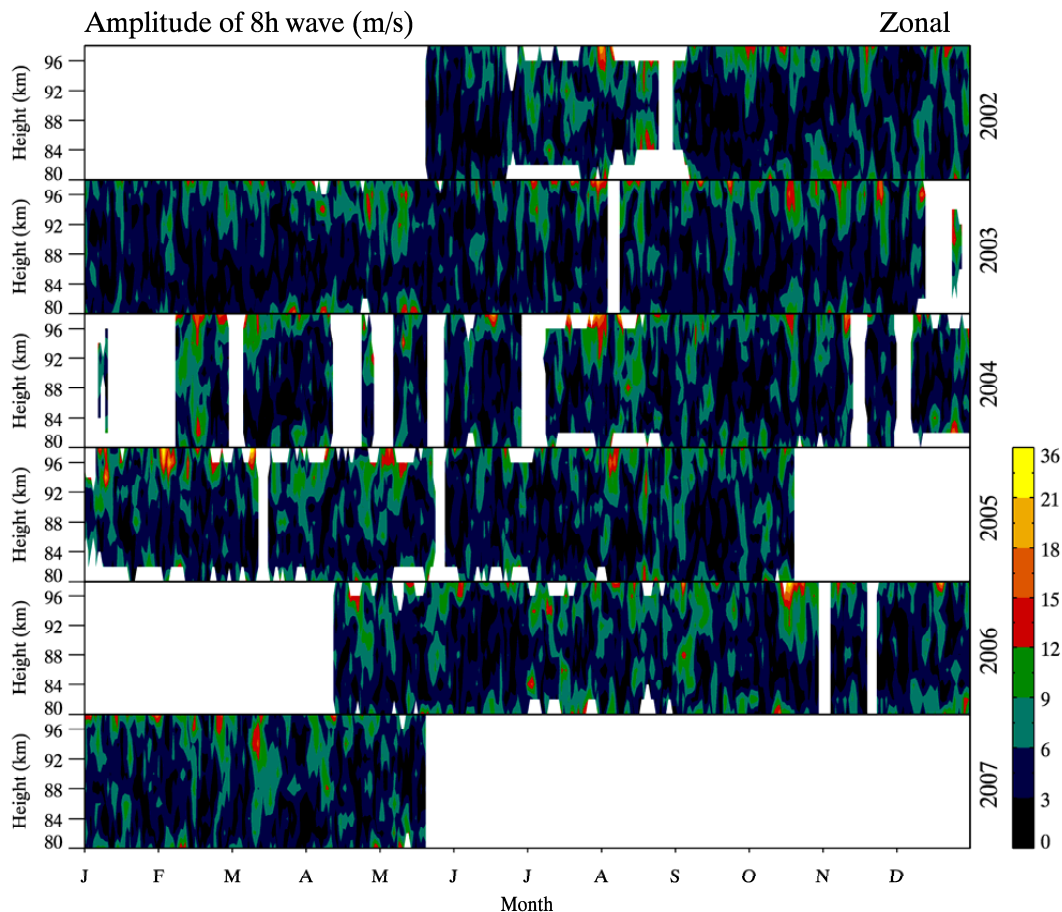


Fig. 4. Same as Fig. 3 but for the zonal wind.

(1) Any gravity waves with periods near 8-h have random phases, hence they would not exhibit coherence over the 5-year long-term interval analyzed in Fig. 2. An incoherent superposition of gravity wave packets would self-cancel and could not produce a narrow peak in a spectrum analysis using a long time series (Younger et al., 2002; Beldon et al., 2006). We conclude that this oscillation can not be classed into the gravity wave category. (2) Lamb waves with periods near 8-h have short lifetimes $\sim 2\text{--}4$ days (Forbes et al., 1999). However, the variation of the 8-h tidal amplitude in the meridional wind (Fig. 3) implies that Maui 8-h wave events generally last much longer than Lamb waves, especially during the equinox months. Thus, the 8-h wave showed in this paper also can not be regarded as Lamb wave. So, the 8-h oscillation in the MLT region over Maui should be interpreted as a tide.

3.2 The seasonal variability of the amplitude and phase of 8-h tide

The most striking feature of the 8-h tide in the MLT region is its intermittent occurrence. Though the amplitude of the 8-h tide is highly variable and does not maintain a large ampli-

tude for long periods of time, its instantaneous amplitude can be as large as the diurnal tide. As mentioned in the introduction of this paper, the 8-h tide has different seasonal variability at different latitudes. For the purpose of studying seasonal variations, we categorize February–April as spring, May–July as summer, August–October as autumn and November–January as winter.

Figures 3 and 4 show the amplitude of the Maui 8-h tide in the meridional wind and zonal wind from 2002 to 2007, respectively. The meridional component of the Maui 8-h tide is significantly stronger than the zonal component. The instantaneous amplitudes can be as large as ~ 36 m/s. During most time intervals, the 8-h tide, especially the zonal component, exhibits the same intermittent behavior that has been observed at mid- and high-latitudes. The exception occurs around spring equinox, when a large amplitude 8-h tide persists for $\sim 40\text{--}50$ days in the meridional wind. Moreover there are many intensive wave events appearing in the meridional wind in autumn months. But in summer and winter months, the 8-h tide is less evident in the MLT region over Maui. From Figs. 3 and 4, we can see that the strongest 8-h tide mainly occurs in the height range of $\sim 88\text{--}98$ km.

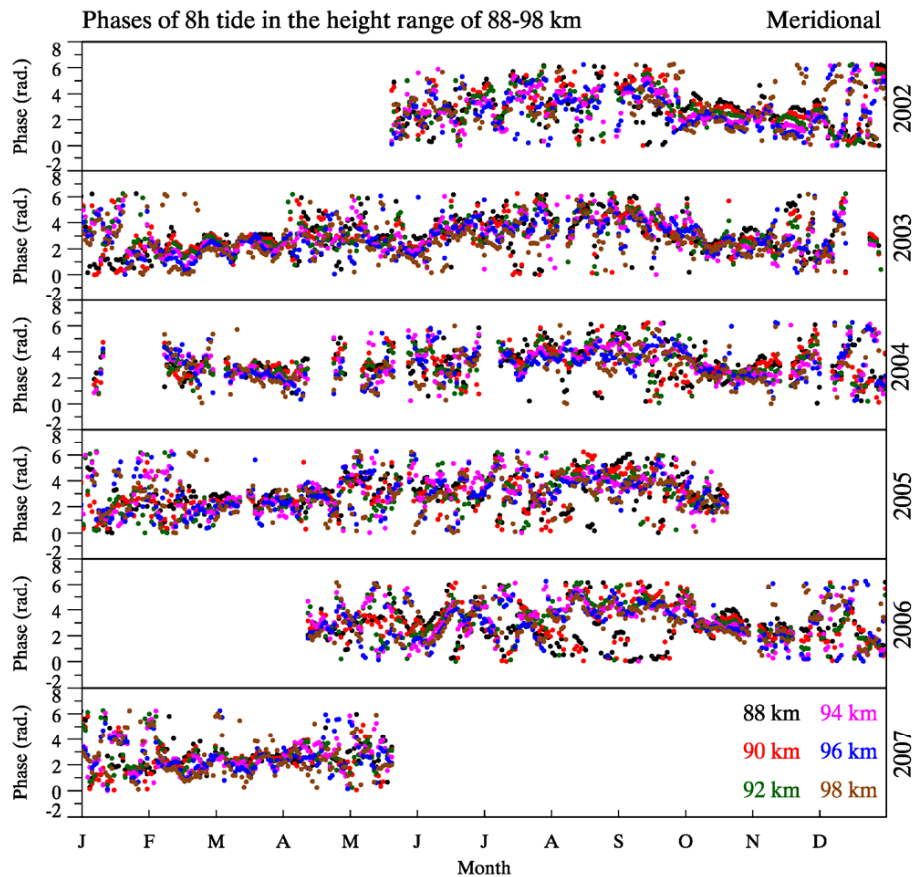


Fig. 5. Phases of the 8-h tide in the meridional wind at 6 height levels 88–98 km, where the 8-h tide has significant amplitude. As shown at the bottom right corner, different colors represent different heights.

Figures 5 and 6 show the variation of the 8-h tidal phase at 6 height levels 88–98 km, where the 8-h tide has significant amplitude. As shown in Fig. 5, near the equinoxes, especially in spring, the phases of the meridional 8-h tide in the height range of 88–98 km are concentrated over a narrow range of values (for example, around 2.5 radian in spring months), indicating high phase coherence during these periods. But, the phase in meridional wind is more irregular in the other months. It should also be noted that the variability of the meridional 8-h tidal phases over Maui is smallest when this wave reaches its strongest amplitudes. However, the zonal component does not seem to exhibit such regular seasonal variations of amplitude and phase (see Figs. 4 and 6).

To show the seasonal variabilities of the 8-h tidal amplitude more clearly, the monthly mean values are calculated from the wind at heights of 88–98 km. The relevant results are revealed in Fig. 7. The monthly mean data are averaged over all years and the error bars indicate the standard deviations of the individual monthly mean values. It is apparent that the meridional component of 8-h tide has maximum amplitude near spring equinox (March) and the second maximum near autumn equinox (October) (see the top of Fig. 7).

However, as shown in the bottom of Fig. 7, the zonal component does not exhibit any significant semiannual variation. Moreover, the meridional component of the monthly mean amplitude is much larger than the zonal component near the equinoxes.

Figure 8 shows the vertical profile of the 8-h tidal amplitude and phase averaged in four seasons. We can see that in all seasons the wave amplitudes in both meridional wind and zonal wind exhibit similar vertical variation, increasing with altitude above 84 km. The seasonal variability of the wave amplitude is also indicated in the two top plots of Fig. 8. The meridional component of Maui 8-h tide has a distinct semiannual feature, strong during spring and autumn but weak during summer and winter, whereas the zonal component does not exhibit significant seasonal variation. The phase profiles showed in the two bottom plots of Fig. 8 indicate that Maui 8-h tide generally has very long vertical wavelengths in all seasons.

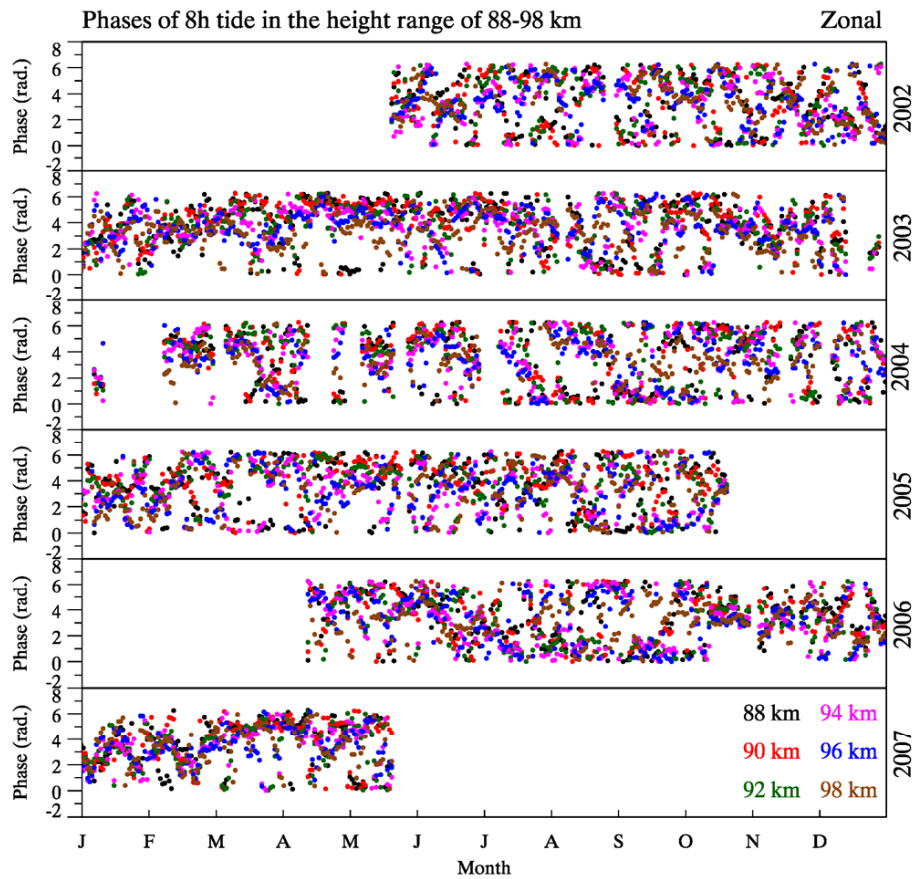


Fig. 6. Same as Fig. 5 but for the zonal wind.

3.3 Altitude dependence of Maui 8-h tide in equinoxes (March and October)

Given that the meridional component of the Maui 8-h tide shows particularly strong wave motion and distinct semianual variation, the meridional wind data in March and October were used to study the altitude dependence of this tide during the equinoxes. Figures 9 and 10 show the altitude dependence of the 8-h tidal amplitude (filled star) and phase (filled circle), respectively. The monthly mean amplitude and phase are calculated from the harmonic fitting method; here, for each month, we chose a 31-day data window centered at the middle of that month. The phase is relevant to the local time when 8-h tide reaches its maximum.

The meridional amplitudes of the 8-h tide at Maui show different altitude variation in March and October. In March, wave amplitudes generally maximize in the height range 92–96 km, e.g. at 94 km in 2003, at 96 km in 2004 and at 92 km in both 2005 and 2007. However, in October the maximum amplitudes appear at the higher altitudes, >96 km. Figure 10 presents the slow downward propagating phase behavior, which indicates that the Maui 8-h tide has upward wave energy flux. Moreover, the phase variation with

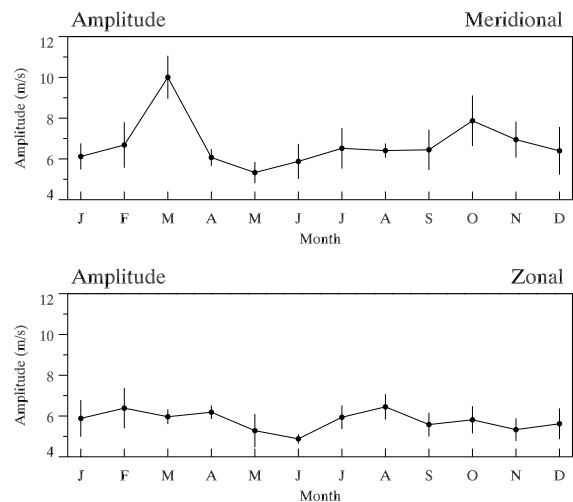


Fig. 7. Climatology of the 8-h tidal amplitude at the heights of 88–98 km using data from 19 May 2002 to 24 May 2007. The error bars indicate the standard deviations of the individual monthly mean values.

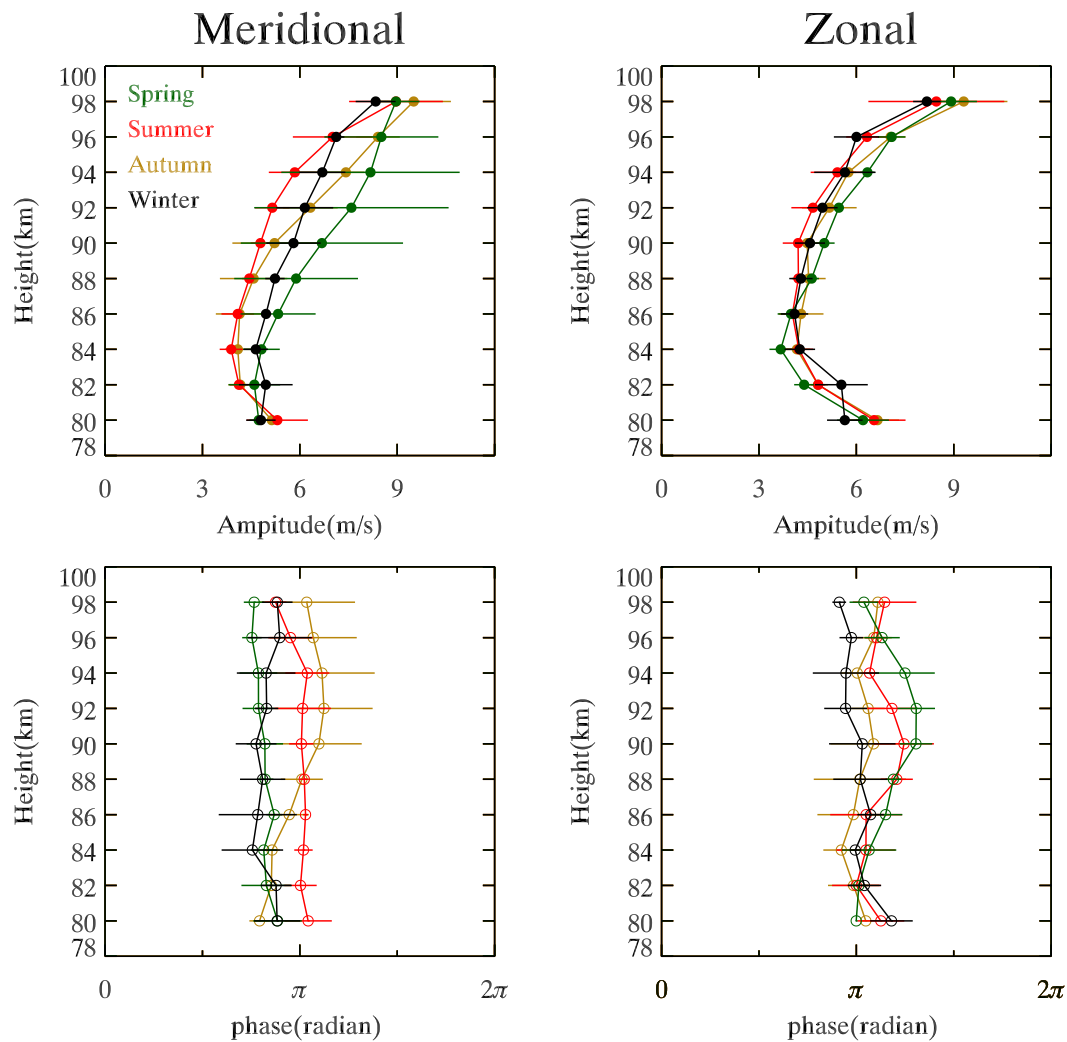


Fig. 8. The vertical profile of the 8-h tidal amplitude (filled circle) and phase (open circle) averaged in four seasons. The left hand is for meridional wind, and the right hand is for zonal wind. The averages are obtained from the monthly-mean 8-h tides. The error bars represent the standard deviation in amplitude, and phase, respectively, of the individual monthly-mean tides.

altitude indicates that the Maui 8-h tide has a long vertical wavelength, for instance, the vertical wavelength ~ 58 km in March 2003, ~ 54 km in March 2007 and longer in other equinox months. These values are in accordance with the model simulation of Smith and Ortland (2001). But, at the low latitude site in the Southern Hemisphere, Cachoeira Paulista (22.7° S, 45° W), the vertical wavelength of the 8-h tide in equinoxes is observed to be ~ 12 – 20 km (Tokumoto et al., 2007). Furthermore, the vertical wavelengths observed at different stations are very different, and range from 12 km to more than 1000 km (Thayaparan, 1997; Namboothiri et al., 2004; Tokumoto et al., 2007). At present, the number of reported studies of the 8-h tide in the MLT region is insufficient for us to clearly understand the temporal and spatial patterns of this wave. Further investigations are greatly needed.

4 Discussion

The meridional component of Maui 8-h tide exhibits semi-annual variations similar to those observed at Cachoeira Paulista (22.7° S, 45° W), a low-latitude station in the Southern Hemisphere (Tokumoto et al., 2007). The 8-h tides at both sites peak near the equinoxes and at higher altitudes. On the other hand, the maximum amplitudes at high-latitude and middle-latitude are observed in autumn and around winter, respectively (Younger et al., 2002; Beldon et al., 2006; Teitelbaum et al., 1989; Thayaparan, 1997; Namboothiri et al., 2004). This indicates that the seasonal behavior of 8-h tide in the MLT region varies with latitude.

Both satellite observation (Smith, 2000) and the model simulation (Akmaev, 2001) showed that the latitudinal distributions of the 8-h tide have a symmetric zonal structure

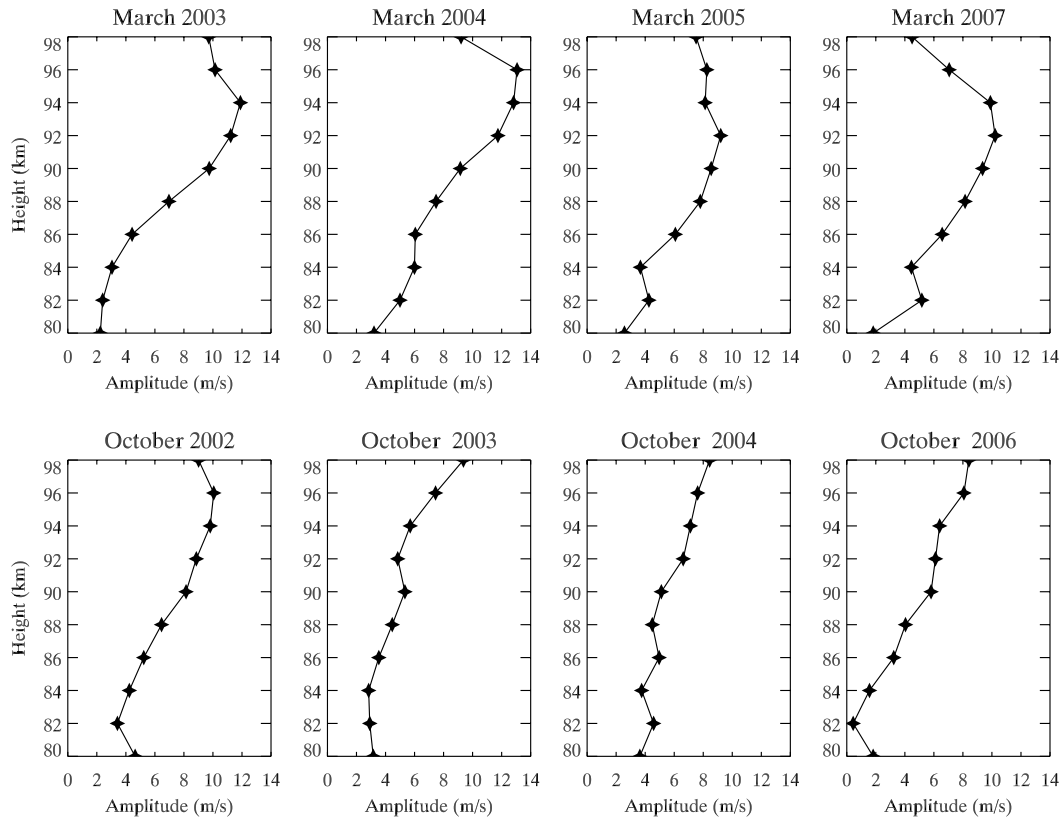


Fig. 9. The vertical profile of Maui 8-h tidal amplitude in March and October in the meridional wind.

and anti-symmetric meridional structure. The annual-mean meridional amplitude of the 8-h tide is substantially weaker than the zonal component as a whole, but near 20° latitude, the 8-h tidal amplitudes have maxima in the meridional component, and weaker motions occur in the zonal component (Fig. 1 of Smith, 2000). The model simulation of Akmaev (2001) showed that the meridional component of the 8-h tide near 20° N is much larger than the zonal component at equinox. As mentioned in Sect. 3, the meridional component of the 8-h tide at Maui (20.75° N) has significantly larger amplitude than the zonal component, which is consistent with the results of Smith (2000) and Akmaev (2001).

Regarding the excitation mechanism for the 8-h tide in the MLT region, the results of the model studies of Smith and Ortland (2001) indicated that direct solar forcing is the dominant mechanism at middle- and high-latitudes, and that nonlinear interaction between diurnal tide and semidiurnal tide contribute to the low-latitude tide. Akmaev (2001) suggested that this nonlinear interaction mainly contributes to the situ excitation of the 8-h tide at 95–100 km, especially during equinox. The wind data observed by the Maui meteor radar are very suitable for studying the mechanisms discussed by Smith and Ortland (2001) and Akmaev (2001). Results of this work will be shown elsewhere.

5 Summary

The mesospheric 8-h tide at a low-latitude station in the Northern Hemisphere has been studied using wind data from the Maui meteor radar (20.75° N, 156.43° W). Our results show that the 8-h tide is a regular and distinct feature in the MLT region over Maui. The instantaneous amplitudes can be large as ~ 36 m/s. The meridional component of this wave is generally larger than the zonal component.

Semiannual variation is the most distinct seasonal feature of the amplitude of the 8-h tide in the meridional wind, which has the first maximum near spring equinox and the second maximum near autumn equinox. The largest monthly mean amplitudes of ~ 9 – 11.5 m/s are observed in the meridional wind in March. On the other hand, the zonal component is irregular and does not exhibit distinct seasonal variability. It is interesting to note that semiannual variation of the 8-h tide is also observed in the MLT region over Cachoeira Paulista (22.7° S, 45° W), a low-latitude station in the Southern Hemisphere, where the 8-h tide also peak at the equinoxes (Tokumoto et al., 2007). At high and middle latitudes of the Northern Hemisphere the mesospheric 8-h tide does not show the semiannual feature (Younger et al., 2002; Beldon et al., 2006; Teitelbaum et al., 1989; Thayaparan, 1997; Namboothiri et al., 2004).

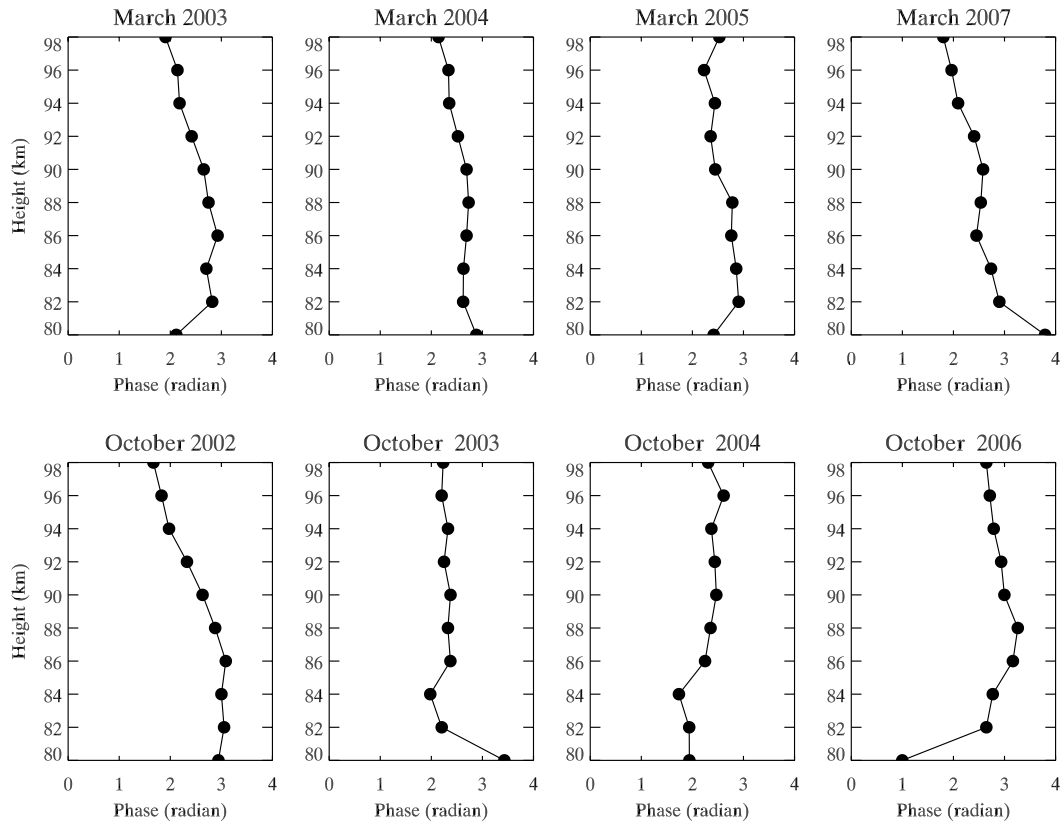


Fig. 10. Same as Fig. 9 but for the phase.

The vertical variation of the Maui 8-h tidal amplitude in the meridional wind shows that the maxima generally appear between 92 km and 96 km in March but at higher altitudes in October. The downward propagating phase indicates that Maui 8-h tide had upward energy flux. The calculated vertical wavelengths of the Maui 8-h tide are typically ≥ 54 km in the equinoxes, when this wave has the largest amplitudes.

Acknowledgements. This research was supported by the National Science Foundation for Post-doctoral Scientists of China (20080440527), the National Science Foundation of China (40804037, 40874080, 40621003, 40674088) and the National Important Basic Research Project (2006CB806306). This project is also supported by the Specialized Research Fund for State Key Laboratories. The Maui meteor radar observations were supported by National Science Foundation grant ATM-0737656.

Topical Editor C. Jacobi thanks two anonymous referees for their help in evaluating this paper.

References

- Akmaev, R. A.: Seasonal variations of the terdiurnal tide in the mesosphere and lower thermosphere: a model study, *Geophys. Res. Lett.*, 28, 3817–3820, 2001.
- Batista, P. P., Clemesha, B. R., Tokumoto, A. S., and Lima, L. M.: Structure of the mean winds and tides in the meteor region over Cachoeira Paulista, Brazil (22.7° S, 45° W) and its comparison with models, *J. Atmos. Sol. Terr. Phys.*, 66, 623–636, 2004.
- Beldon, C. L., Muller, H. G., and Mitchell, N. J.: The 8-hour tide in the mesosphere and lower thermosphere over the UK, 1988–2004, *J. Atmos. Sol. Terr. Phys.*, 68, 655–668, 2006.
- Forbes, J. M., Palo, S. E., and Zhang, X.: Lamb waves in the thermosphere: observational evidence and global consequences, *J. Geophys. Res.*, 104(A), 17107–17115, 1999.
- Franke, S. J., Chu, X. Liu, A. Z., and Hocking, W. K.: Comparison of meteor radar and Na Doppler lidar measurements of winds in the mesopause region above Maui, Hawaii, *J. Geophys. Res.*, 110, D09S02, doi:10.1029/2003JD004486, 2005.
- Fritts, D. C. and Isler, J. R.: Mean motions and tidal and two-day structure and variability in the mesosphere and lower thermosphere over Hawaii, *J. Atmos. Sci.*, 51, 2145–2164, 1994.
- Hocking, W. K. and Thayaparan, T.: Simultaneous and collocated observation of winds and tides by MF and meteor radar over London, Canada, *Radio Sci.*, 32(2), 833–865, 1997.
- Hocking, W. K., Fuller, B., and Vandeppeer, B.: Real-time determination of meteor-related parameters utilizing modern digital technology, *J. Atmos. Sol. Terr. Phys.*, 63, 155–169, 2001.
- Lomb, N. R.: Least-squares frequency analysis of unequally spaced data, *Astrophys. Space Sci.*, 39, 447–462, 1976.
- Manson, A. H. and Meek, C. E.: Dynamics of the middle atmosphere at Saskatoon (52 N, 107 W): A spectral study during 1981, 1982, *J. Atmos. Terr. Phys.*, 48, 1039–1055, 1986.
- Namboothiri, S. P., Kishore, P., Murayama, Y., and Igarashi, K.:

- MF radar observations of terdiurnal tide in the mesosphere and lower thermosphere at Wakkanai (45.4° N, 141.7° E), Japan, *J. Atmos. Sol. Terr. Phys.*, 66, 241–250, 2004.
- Pendleton Jr., W. R., Taylor, M. J., and Gardner, L. C.: Terdiurnal oscillations in OH Meinel rotational temperatures for fall conditions at northern midlatitude sites, *Geophys. Res. Lett.*, 27, 1799–1802, 2000.
- Scargle, J. D.: Studies in astronomical time series analysis. II, Statistical aspects of spectral analysis of unevenly spaced data, *Astrophys. J.*, 263, 835–853, 1982.
- Smith, A. K.: Structure of the terdiurnal tide at 95 km, *Geophys. Res. Lett.*, 27, 177–180, 2000.
- Smith, A. K. and Ortland, D. A.: Modeling and analysis of the structure and generation of the terdiurnal tide, *J. Atmos. Sci.*, 58, 3116–3134, 2001.
- Taori, A., Taylor, M. J., and Franke, S.: Terdiurnal wave signatures in the upper mesospheric temperature and their association with the wind field at low latitudes (20° N), *J. Geophys. Res.*, 110, D09S06, doi:10.1029/2004JD004564, 2005.
- Teitelbaum, H., Vial, F., Manson, A. H., Giraldez, R., and Massebeuf, M.: Non-linear interaction between the diurnal and semidiurnal tides: Terdiurnal and diurnal secondary waves, *J. Atmos. Terr. Phys.*, 51, 627–634, 1989.
- Thayaparan, T.: The terdiurnal tide in the mesosphere and lower thermosphere over London Canada (43° N, 81° W), *J. Geophys. Res.*, 102, 21695–21708, 1997.
- Tokumoto, A. S., Batiata, P. P., and Clemesha, B. R.: Terdiurnal tides in the MLT region over Cachoeira Paulista (22.7° S, 45° W), *Revista Brasileira de Geofísica*, 25, 69–78, 2007.
- Younger, P. T., Pancheva, D., Middleton, H. R., and Mitchell, N. J.: The 8-h tide in the Arctic mesosphere and lower thermosphere, *J. Geophys. Res.*, 107(A12), 1420, doi:10.1029/2001JA005086, 2002.
- Zhao, G., Liu, L., Ning, B., Wan, W., and Xiong, J.: The terdiurnal tide in the mesosphere and lower thermosphere over Wuhan (30° N, 114° E), *Earth Planets Space*, 57, 393–398, 2005.